Supersymmetry, dark matter and the LHC

GGI Conference: The Dark Matter connection: Theory & Experiment

May 20, 2010

[PN]

Outline

- Connection of DM to LHC with LSP= χ^0

  Other LHC and dark matter related talks: By Dutta, Kraml, Polesello, Su
- Gaugino-Higgsino content of the neutralino and LHC signatures
- Multicomponent dark matter.

Available online at www.sciencedirect.com
ScienceDirect
Nuclear Physics B (Proc. Suppl.) 200–202 (2010) 185–417
NUCLEAR PHYSICS B PROCEEDINGS SUPPLEMENTS
www.elsevier.com/locate/npbps

The Hunt for New Physics at the Large Hadron Collider

Principal Conveners: Pran Nath[a]
Brent Nelson[a]

Conveners for New Physics Sections: Hooman Davoudiasl[b] (Extra Dimensions)
Bhaskar Dutta[c] (Dark Matter)
Daniel Feldman[d] and Zuowei Liu[e] (Hidden Sectors)
Tao Han[f] (Top)
Paul Langacker[g] (Z Prime)
Rabi Mohapatra[h] and Jose Valle[i] (Neutrinos)
Pran Nath[a] (SUSY)
Brent Nelson[a] (Strings)
Apostolos Pilaftsis[j] (CP violation)
Dirk Zerwas[k] (Higgs)

Shehu AbdusSalam[l,bc], Claire Adam-Bourdarios[k], J.A. Aguilar-Saavedra[m], Benjamin Allanach[l], B. Altunkaynak[a], Luis A. Anchordoqui[n], Howard Baer[o], Borut Bajc[p], O. Buchmueller[q], M. Carena[r,s], R. Cavanaugh[t,u], S. Chang[v], Kiwoon Choi[w], C. Csáki[x], S. Dawson[b], F. de Campos[y], A. De Roeck[q,z], M. Dührssen[aa], O.J.P. Éboli[ab], J.R. Ellis[q], H. Flächer[q], H. Goldberg[a], W. Grimus[ac], U. Haisch[ad], S. Heinemeyer[ae], M. Hirsch[i], M. Holmes[a], Tarek Ibrahim[af], G. Isidori[ag], Gordon Kane[d], K. Kong[ah], Remi Lafaye[ai], G. Landsberg[aj], L. Lavoura[ak], Jae Sik Lee[al], Seung J. Lee[am], M. Lisanti[ah], Dieter Lüst[an,ao], M.B. Magro[ap], R. Mahbubani[t], M. Malinsky[aq], Fabio Maltoni[ar], S. Morisi[i], M.M. Mühlleitner[as], B. Mukhopadhyaya[at], M. Neubert[ad], K.A. Olive[au], Gilad Perez[am], Pavel Fileviez Pérez[f], T. Plehn[av], E. Pontón[aw], Werner Porod[ax], F. Quevedo[l,bc], M. Rauch[as], D. Restrepo[ay], T.G. Rizzo[ah], J. C. Romão[ak], F.J. Ronga[az], J. Santiago[m], J. Schechter[bb], G. Senjanović[bc], J. Shao[bb], M. Spira[bd], S. Stieberger[an], Zack Sullivan[be], Tim M.P. Tait[bf], Xerxes Tata[f,bg], T.R. Taylor[a], M. Toharia[h], J. Wacker[ah], C.E.M. Wagner[s,bh,bi], Lian-Tao Wang[bj], G. Weiglein[bk], D. Zeppenfeld[as], K. Zurek[d]

SUSY breaking mechanisms

- Gravity mediation (1982)

  Chamseddine, Arnowitt, PN (1982)
  Barbieri, Ferrara, Savoy (1982)

  Hall, Lykken, Weinberg (1983)

- Gauge mediation (1994)

  Dine, Nelson, Shirman, $\cdots$

- Anomaly mediation (1999)

  Randall, Sundrum, $\cdots$

- Mixed gravity, anomaly, gauge mediation such as mirage, deflected mirage etc.

Connection of DM to LHC with LSP= χ

Typically the satisfaction of the relic density constraints are satisfied in four broad regions of the SUGRA parameter space.

- Bulk regions
- Pole regions
- Coannihilation regions
  Wino, stau, stop, gluino $\cdots$ coannihilation
- Hyperbolic Branch/Focus Point region
  Chan, Chattopadhyay, PN (1998), Feng, Matchev, Moroi (2000); Baer, Tata et.al. (2003)

These regions could possibly lead to distinguishable signatures at the LHC. We explore this possibility specifically for the stau coannihilation region and for for the HB/FP region.

At the LHC:
Some Prominent SUSY signatures

In pp collisions at the LHC one will produce $\tilde{g}\tilde{g}, \tilde{g}\tilde{q}, \tilde{q}\tilde{q}$. The $\tilde{g}, \tilde{q}$ that are produced will decay producing many signatures

$$\tilde{g} \to q\tilde{q}, \quad q\bar{q}\tilde{\chi}_i^0, \quad q\bar{q}'\tilde{\chi}_j^{\pm}$$
$$\tilde{q} \to q\tilde{g}, \quad q\tilde{\chi}_i^0, \quad q'\tilde{\chi}_j^{\pm}$$

$\chi_i^0, \chi_j^{\pm}$ will decay producing in general multi-leptons and the LSP neutralino will carry large missing energy.

Typical SUSY signals: Jets + leptons+ E_T^{miss}.

1. One lepton+jets+E_T^{miss}.
2. Opposite sign (OS) dileptons +jets+E_T^{miss}.
3. Same sign (SS) dileptons +jets+E_T^{miss}.
4. 3leptons + jets+E_T^{miss}.
5. Tagged b jets and tau jets with and without missing E_T.

Post Trigger Level Cuts

1. In an event, we only select photons, electrons, and muons that have transverse momentum $P_T^p > 10$ GeV and $|\eta^p| < 2.4$, $p = (\gamma, e, \mu)$.
2. Taus which satisfy $P_T^\tau > 10$ GeV and $|\eta^\tau| < 2.0$ are selected.
3. For hadronic jets, only those satisfying $P_T^j > 60$ GeV and $|\eta^j| < 3$ are selected.
4. We require a large amount of missing transverse momentum, $P_T^{miss} > 200$ GeV.
5. There are at least two jets that satisfy the P_T and η cuts.

The default post trigger level cuts are standard and are designed to suppress the Standard Model background, and highlight the SUSY events over a broad class of models.

Stau Coannihilation and Hyperbolic/Focus point region and Decay Chains

- On HB/FP the squarks are generally heavy and thus the gluinos are produced more profusely in this region than squarks. The gluinos have longer decay chains and thus missing P_T associated with this region is smaller.

$$\tilde{g} \longrightarrow q\bar{q}\tilde{\chi}_i^0, \quad q\bar{q}'\tilde{\chi}_j^{\pm}$$

  Also a larger multiplicity of quarks, specfically b quarks, produced in the HB/FP region.

- On the Stau co-annihilation branch squarks are light and they are more profusely produced than gluinos. The squarks have shorter decay chains, and thus missing P_T associated with this region is larger.

$$\tilde{q} \longrightarrow q\tilde{\chi}_i^0, \quad q'\tilde{\chi}_j^{\pm}$$

What can we learn from the LHC regarding the origin of Dark matter?

Feldman, Liu, PN: Phys. Rev. D 78, 083523 (2008), arXiv:0808.1595 [hep-ph]

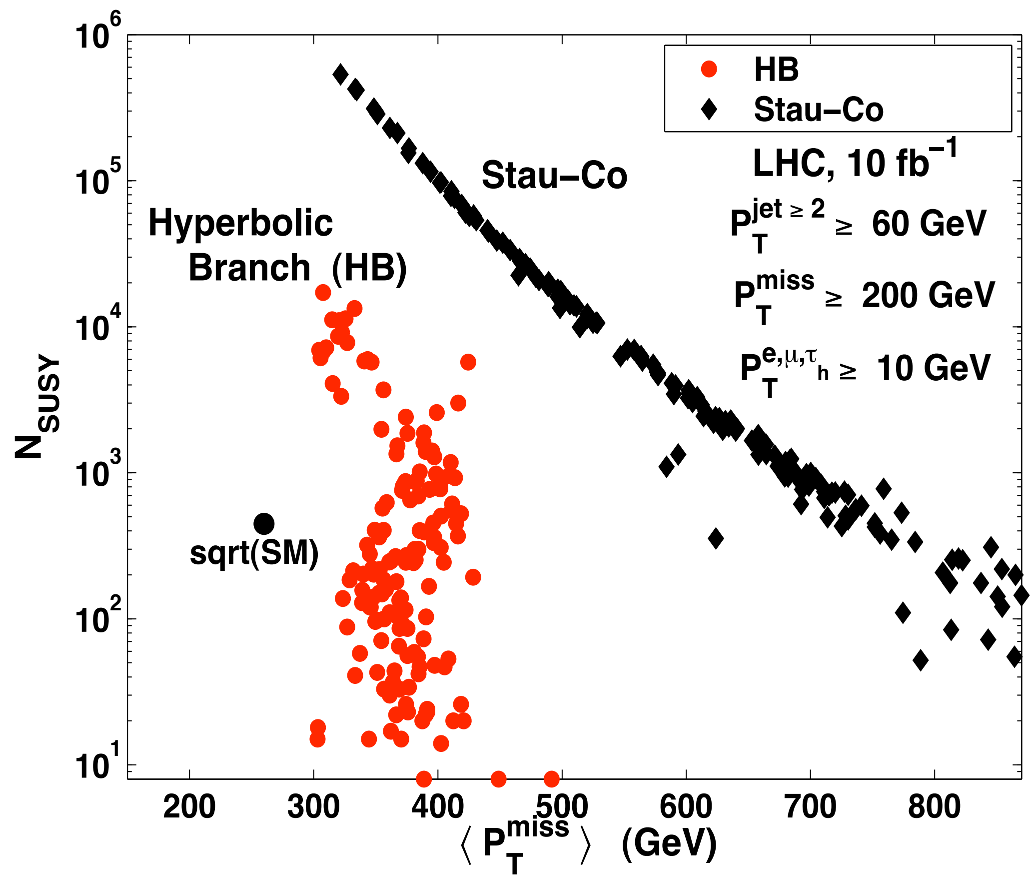

Figure: N_{SUSY} vs. $\langle P_T^{\mathrm{miss}} \rangle$ for each parameter point in the Stau-Co and HB. $\langle P_T^{\mathrm{miss}} \rangle$ acts as an indicator of Stau-Co and HB regions.

Feldman, Liu, PN: Phys. Rev. D 78, 083523 (2008), arXiv:0808.1595 [hep-ph]

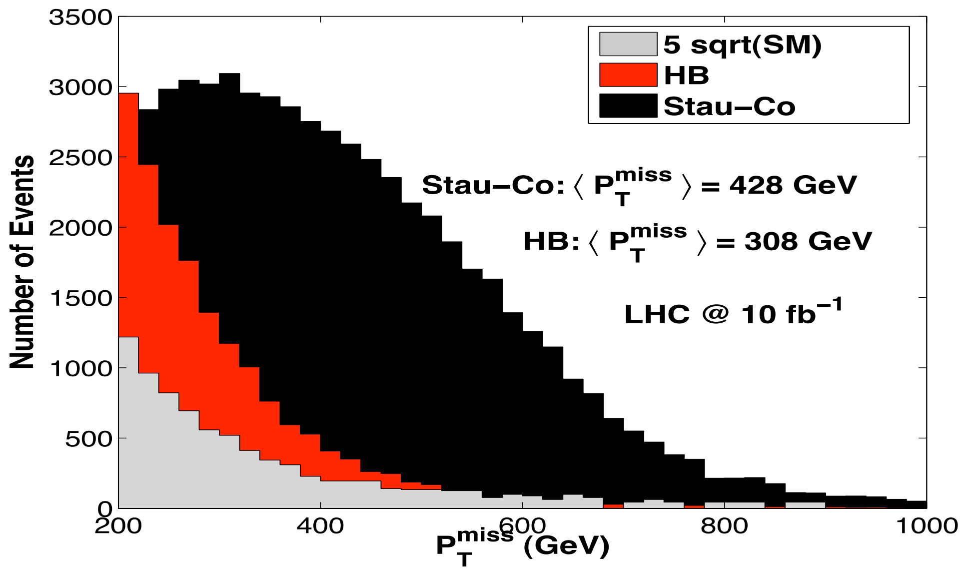

Feldman, Liu, PN: Phys. Rev. D 78, 083523 (2008), arXiv:0808.1595 [hep-ph]

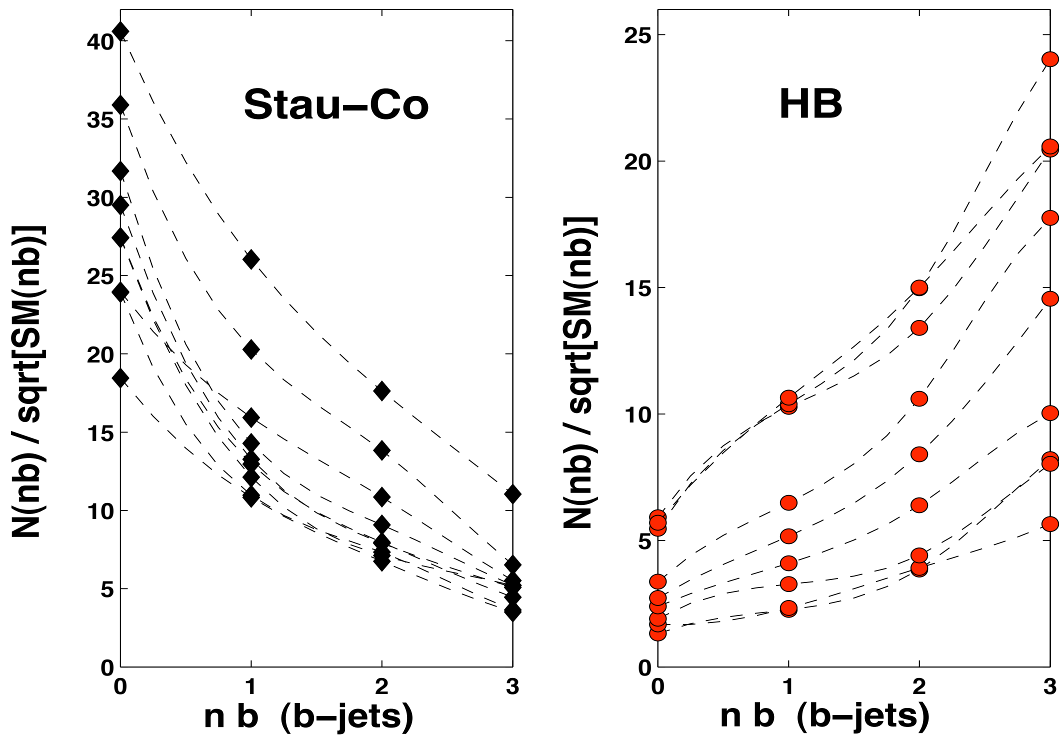

Figure: $N(nb)/\sqrt{\mathrm{SM}(nb)}$ vs nb for the Stau-Co and HB regions where $N(nb)$ (SM(nb)) is the number of SUSY (SM) events that contain n b-tagged jets. A sharp discrimination between the Stau-Co and the HB by b-tagging is observed. The number n^*_{jet} is fixed at 2. Here $m_{\tilde{g}} \leq 1.1$ TeV.

Direct detection and NLSP

Feldman, Liu, PN, arXiv:0711.4591 [hep-ph]; PLB 662,190(2008)

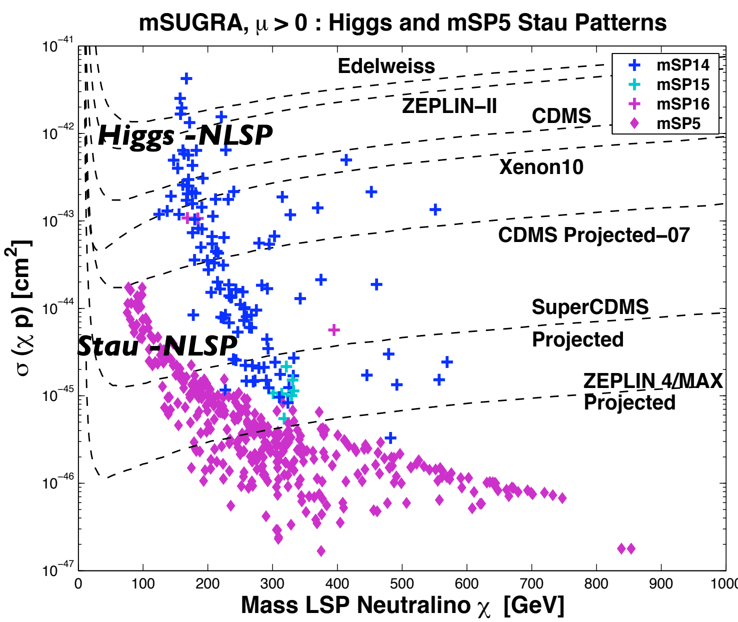

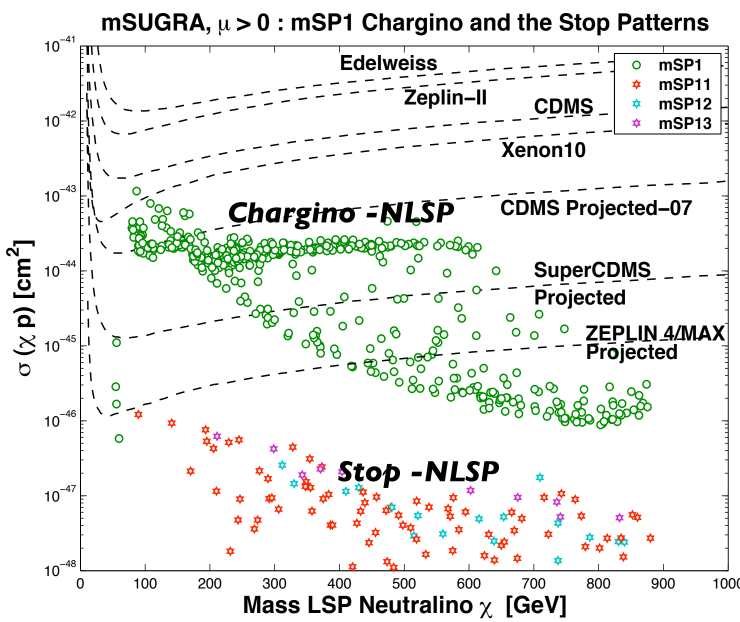

The Wall: Chattopadhyay, Corsetti, PN (2003); Baer, Balazs, Belyaev, O,Farril (2003); Roszkowski, Ruiz de Austri, Trotta (2007).
Chargino Wall: Feldman, Liu, PN (2008)

Combined LHC and dark matter data

Feldman, Liu, PN: Phys. Rev. D 78, 083523 (2008), arXiv:0808.1595 [hep-ph]

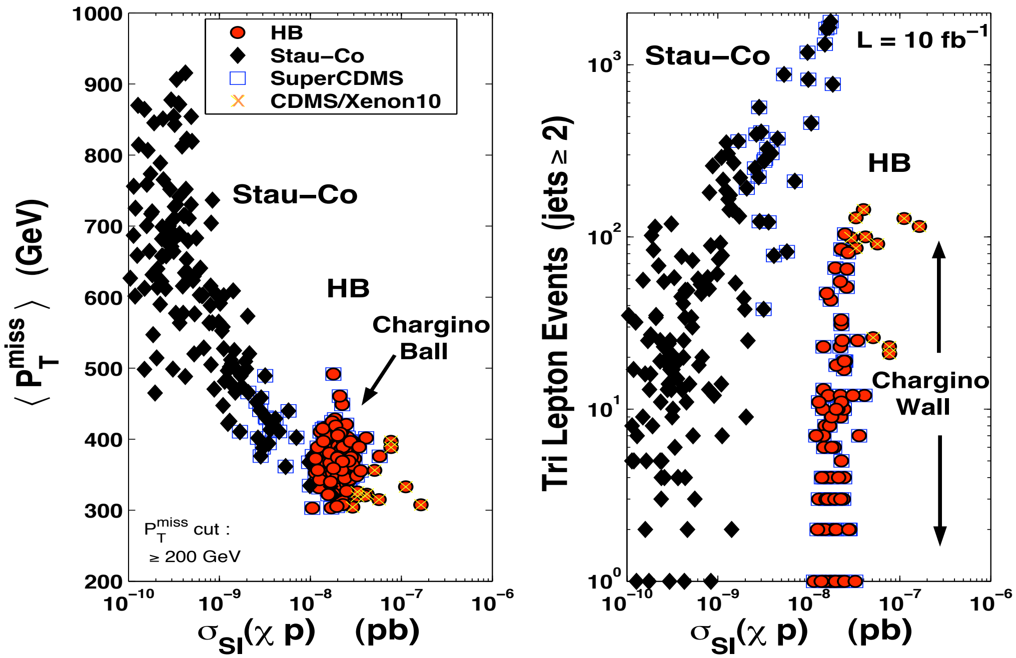

Feldman, Liu, PN: JHEP 0804:054,2008.

40 counting signatures for each parameter point.

40 Signatures	Description	40 Signatures	Description
(1) — 0L	0 Lepton	(22)—0T	0 τ
(2)—1L	1 Lepton	(23)—1T	(23)—1 τ
(3)—2L	2 Lepton	(24)—2T	(24)—2 τ
(4)—3L	3 Lepton	(25)—3T	(25)—3 τ
(5)—4L	4 Lepton and more	(26)—4T	4 τ and more
(6)—0L1b	0 Lepton + 1 b-jet	(27)—0T1b	0 τ + 1 b-jet
(7)—1L1b	1 Lepton + 1 b-jet	(28)—1T1b	1 τ + 1 b-jet
(8)—2L1b	2 Lepton + 1 b-jet	(29)—2T1b	2 τ + 1 b-jet
(9)—0L2b	0 Lepton + 2 b-jet	(30)—0T2b	0 τ + 2 b-jet
(10)—1L2b	1 Lepton + 2 b-jet	(31)—1T2b	1 τ + 2 b-jet
(11)—2L2b	2 Lepton + 2 b-jet	(32)—2T2b	2 τ + 2 b-jet
(12)—ep	e^+ in 1L	(33)—em	e^- in 1L
(13)—mp	μ^+ in 1L	(34)—mm	μ^- in 1L
(14)—tp	τ^+ in 1T	(35)—tm	τ^- in 1T
(15)—OS	Opposite Sign Di-Lepton	(36)—0b	0 b-jet
(16)—SS	Same Sign Di-Lepton	(37)—1b	1 b-jet
(17)—OSSF	Opp Sign Same Flavor Di-Lepton	(38)—2b	2 b-jet
(18)—SSSF	Same Sign Same Flavor Di-Lepton	(39)—3b	3 b-jet
(19)—OST	Opposite Sign Di-τ	(40)—4b	4 b-jet and more
(20)—SST	Same Sign Di-τ		
((21)—TL	1 τ plus 1 Lepton		

Feldman, Liu, PN: JHEP 0804:054,2008.

Kinematical signatures
1. P_T^{miss}
2. P_T peak value
3. Effective Mass $= P_T^{miss} + \sum_j P_T^j$
4.Invariant Mass of all jets
5.. Invariant Mass of e^+e^- pair
6. Invariant Mass of $\mu^+\mu^-$ pair
7. Invariant Mass of $\tau^+\tau^-$ pair

A list of the kinematical signatures analyzed for each point in the SUGRA model parameter space. $L = e, \mu$ signifies only electrons and muons.

OSSF Di-lepton

Feldman, Liu, PN: JHEP 0804:054,2008.

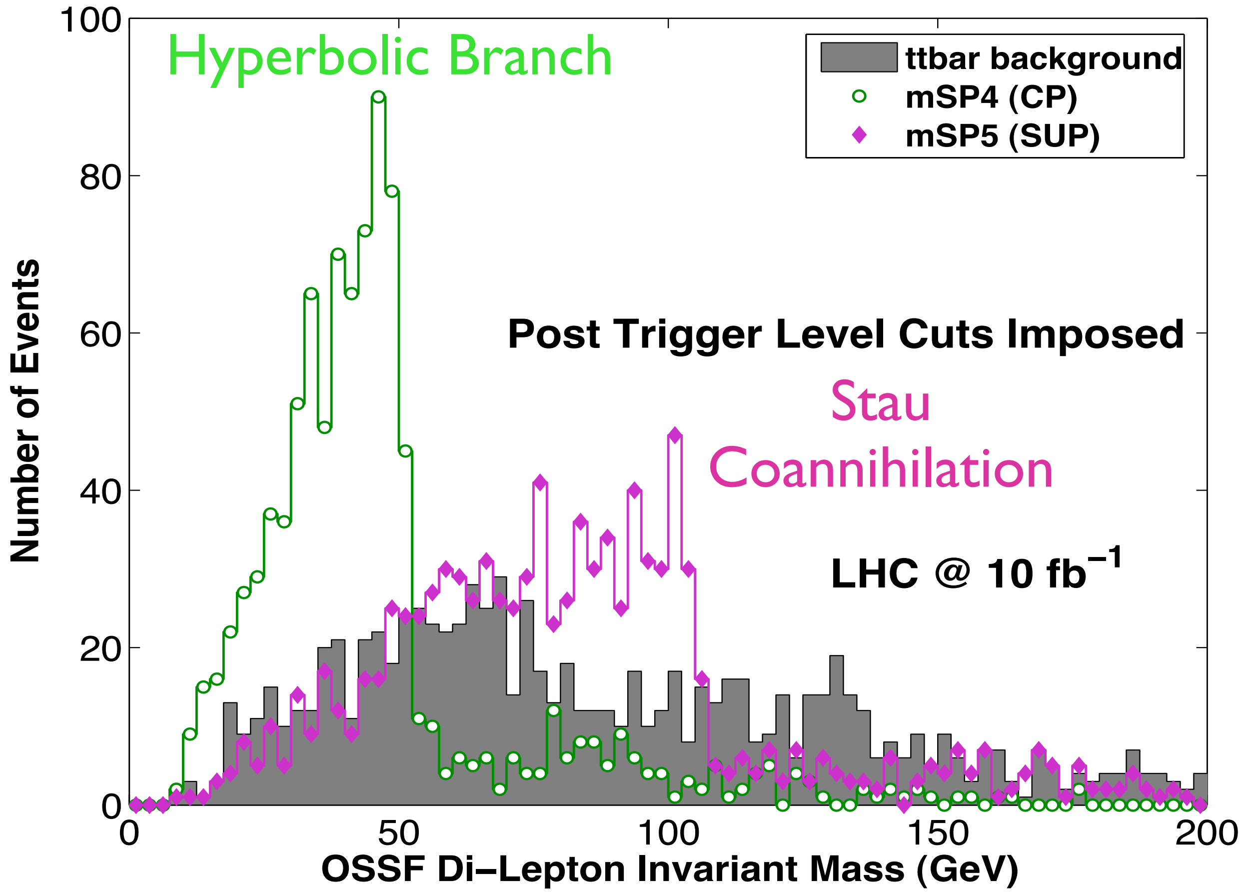

Feldman, Liu, PN: JHEP 0804:054,2008.

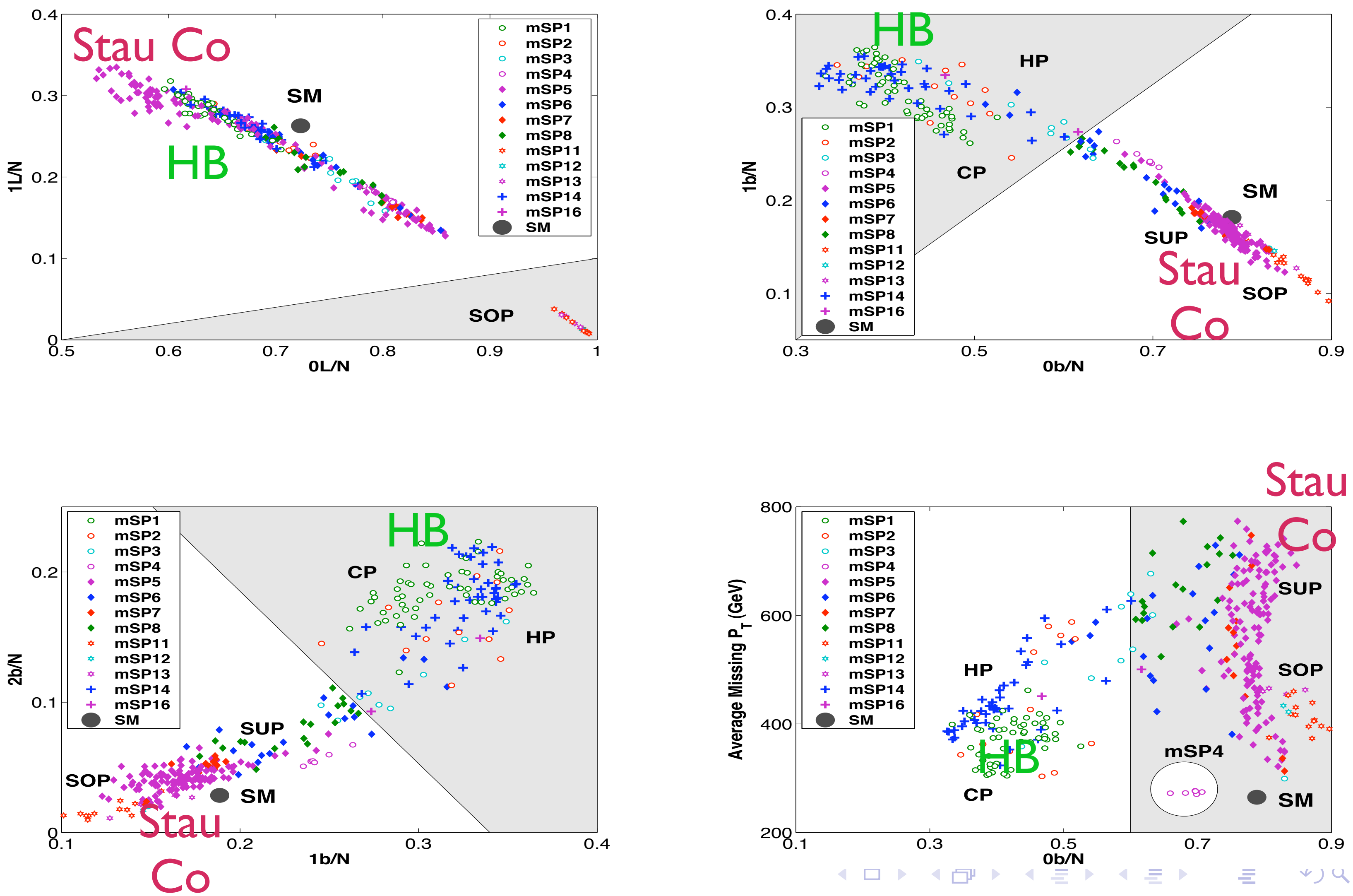

SUSY: like-sign dileptons

From Conway's talk at Pheno 2010

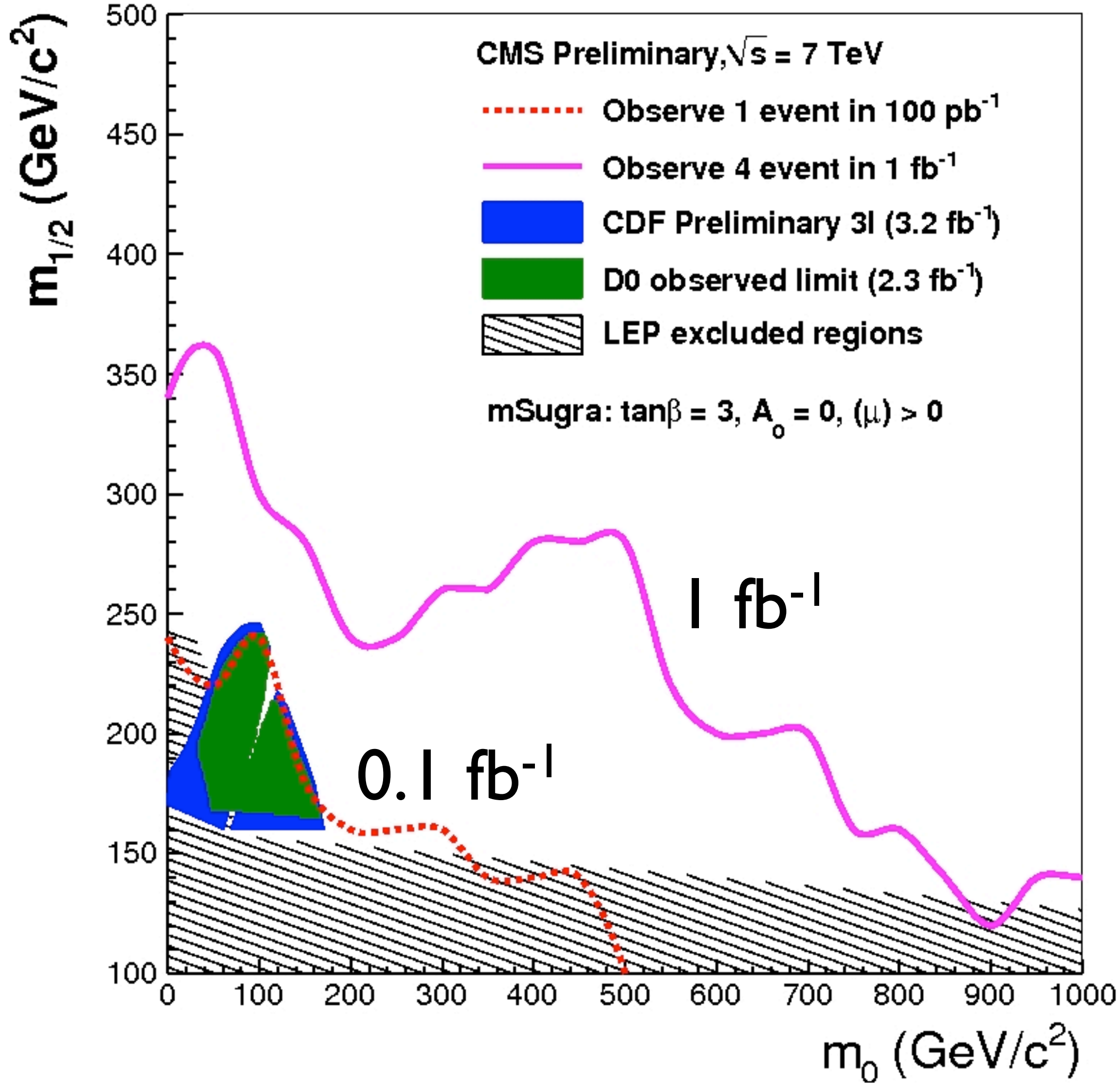

Similar sensitivity seen in like-sign dilepton analysis

Very soon the LHC will surpass the Tevatron in the search for SUSY

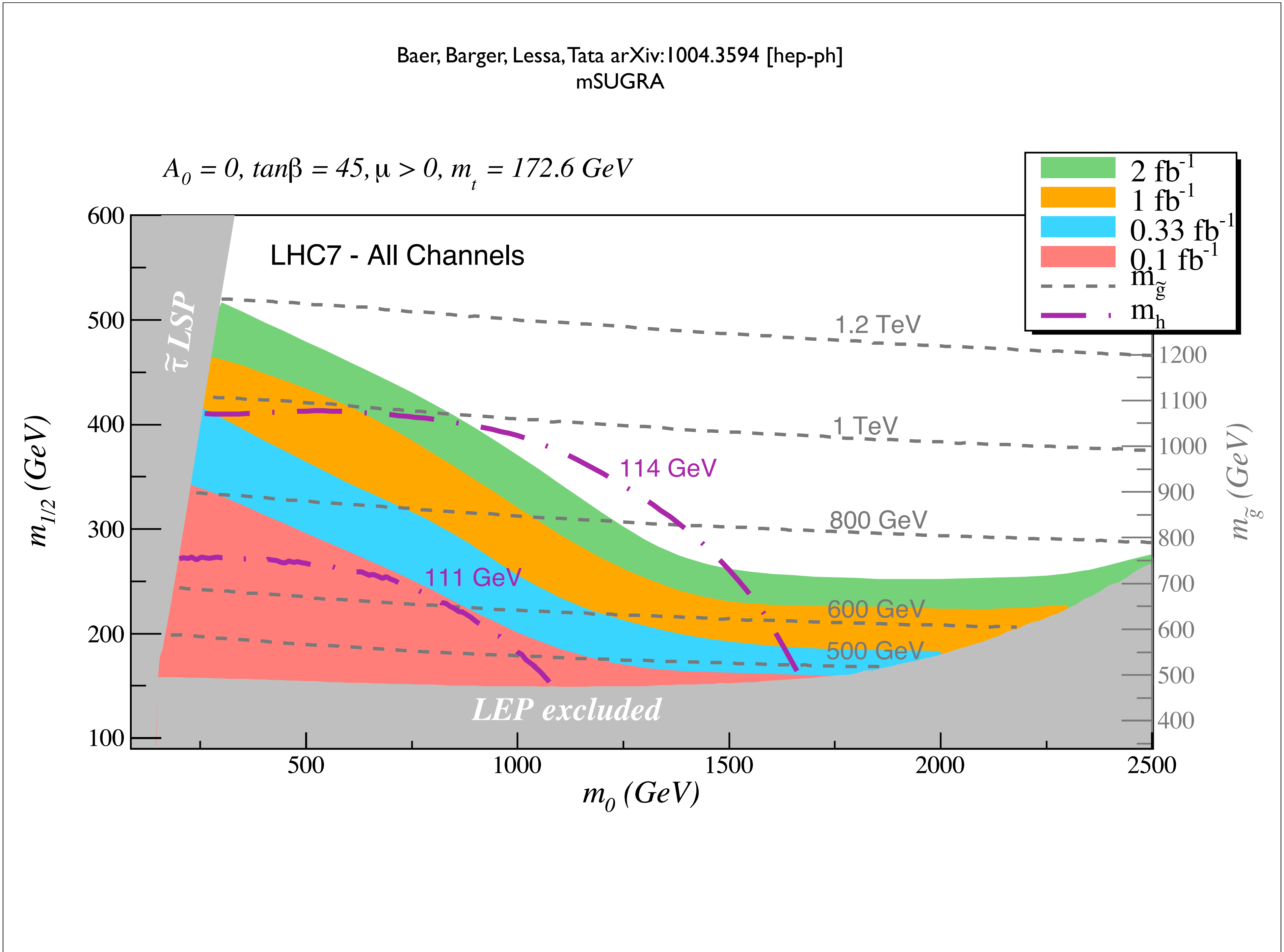

Baer, Barger, Lessa, Tata arXiv:1004.3594 [hep-ph]
mSUGRA
$A_0 = 0, \tan\beta = 45, \mu > 0, m_t = 172.6$ GeV
LHC7 - All Channels
$\tilde{\tau}$ LSP
LEP excluded
2 fb^{-1}
1 fb^{-1}
0.33 fb^{-1}
0.1 fb^{-1}
$m_{\tilde{g}}$
m_h
1.2 TeV
1 TeV
800 GeV
600 GeV
500 GeV
114 GeV
111 GeV
$m_{1/2}$ (GeV)
m_0 (GeV)
$m_{\tilde{g}}$ (GeV)

Gaugino -Higgsino Content of the Neutralino and LHC Signatures

The signatures at the LHC will be dependent on the gaugino vs higgsino content of the neutralino. Thus the neutralino wave function can be expanded as

$$\chi = \alpha\tilde{\lambda}_B + \beta\tilde{\lambda}_W + \gamma\tilde{h}_1 + \delta\tilde{h}_2$$

For illustration we consider two models.

- Model 1: A pure Wino model (PWM) where the neutralino is almost 100% wino. Models of this type arise in anomaly mediated breaking. One characteristic of such models is that the lighter chargino and the neutralino are essentially degenerate.
- Model 2: As second example we consider a mixed Higgino-Wino model (HWM) which has a substantial higgsino component.

These models lead to distinguishable signatures at the LHC.

Pure Wino and Higgsino-Wino model examples

- Pure Wino Model (PWM)
  - $(m_0, m_{1/2}, A_0, \tan\beta) = (1000, 850, 0, 10)$,
  - $(\delta_{1,2,3}, \text{sign}\mu) = (0, -.7, 0, +)$.

$$\tilde{\chi}^0 = .009\lambda_B - 0.996\lambda_W + .081\tilde{h}_1 - .023\tilde{h}_2$$

- Higgsino-wino model (HWM)
  - $(m_0, m_{1/2}, A_0, \tan\beta) = (800, 558, 0, 5)$,
  - $(\delta_{1,2,3}, \text{sign}\mu) = (-0.09, -.5, -.51, +)$.

$$\tilde{\chi}^0 = .726\lambda_B - 0.616\lambda_W + .26\tilde{h}_1 - .16\tilde{h}_2$$

Sparticle masses in mixed Higgsino-Wino and Pure Wino models

Feldman, Liu, PN, Nelson, PRD D 80, 075001 (2009)

Mass	HWM	PWM		Mass	HWM	PWM
$m_{\tilde{\chi}_1^0}$	198.9	195.2		$m_{\tilde{t}_1}$	648.5	1516
$m_{\tilde{\chi}_2^0}$	217.0	357.0		$m_{\tilde{t}_2}$	866.8	1749
$m_{\tilde{\chi}_3^0}$	429.9	1025		$m_{\tilde{b}_1}$	841.4	1729
$m_{\tilde{\chi}_4^0}$	451.3	1029		$m_{\tilde{b}_2}$	970.2	1902
$m_{\tilde{\chi}_1^\pm}$	208.8	195.5		$m_{\tilde{\tau}_1}$	817.7	1011
$m_{\tilde{\chi}_2^\pm}$	448.6	1036		$m_{\tilde{\tau}_2}$	822.8	1041
$m_{\tilde{g}}$	707.1	1929				

Relevant sparticle mass spectra for the HWM and PWM as calculated from the high-scale boundary conditions. All masses are in GeV.

Effective mass distribution

Feldman, Liu, PN, Nelson, PRD D 80, 075001 (2009)

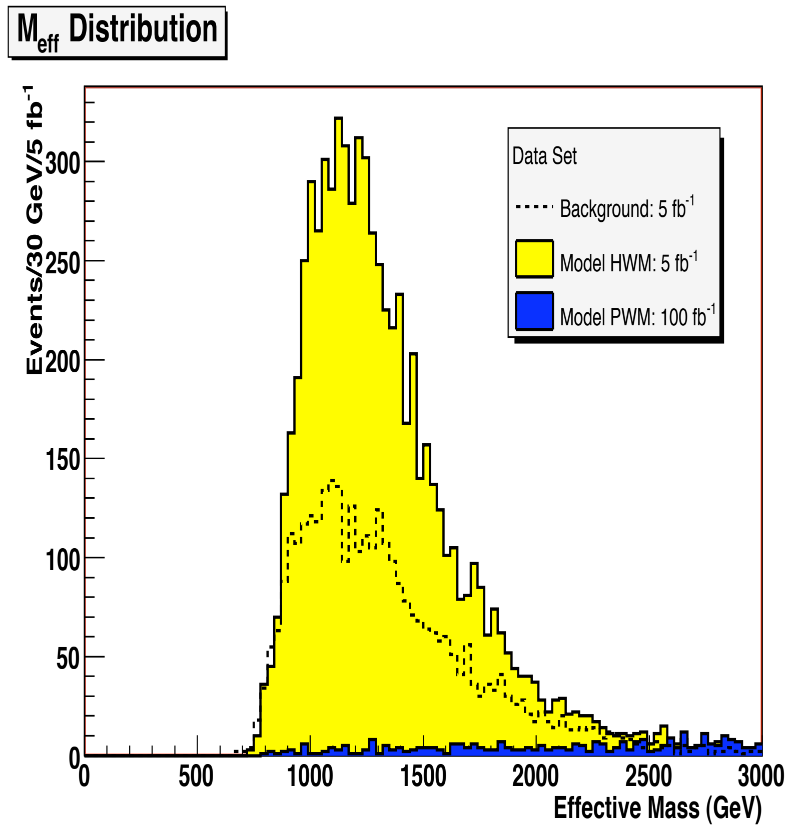

M_{eff} is defined as the scalar sum of the transverse momenta of four hardest jets $P_T \geq (200, 150, 50, 50)$ GeV in the event plus missing energy ($E_T^{miss} \geq 200$ GeV).The plot is of events for the Higgsino-Wino model (for 5fb^{-1} yellow) and for Pure Wino model (100 fb^{-1} blue).

The invariant mass distribution of two b-jets events in Higgsino-Wino model.

Feldman, Liu, PN, Nelson, PRD D 80, 075001 (2009)

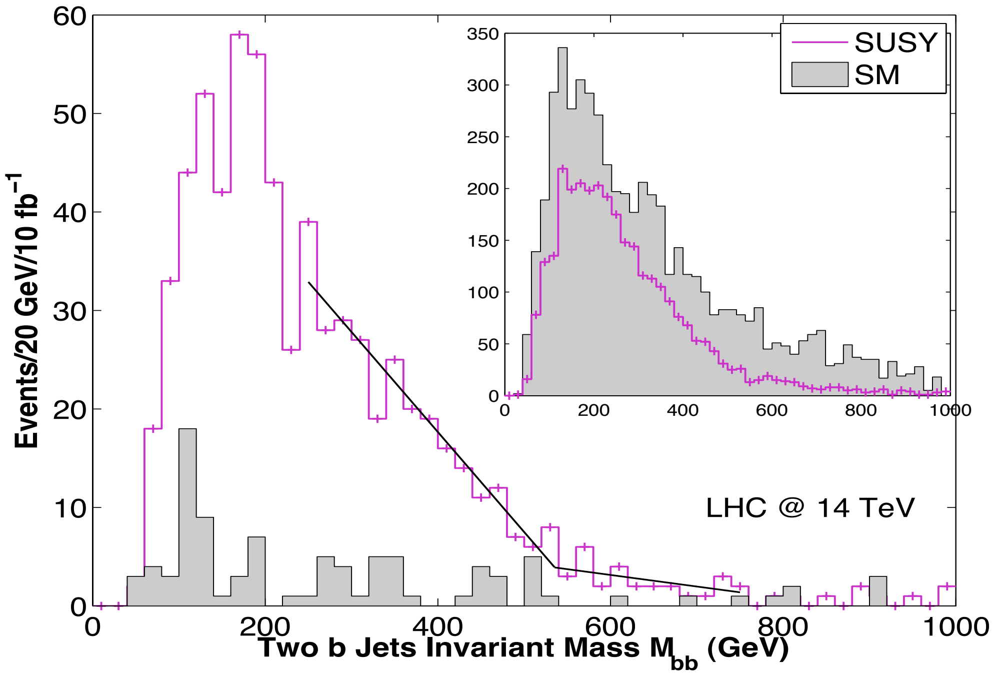

In HWM gluino is light and will be produced in significant amounts at the LHC. Now $\tilde{g} \longrightarrow b\bar{b} + \tilde{\chi}^0$, and so $m_{\tilde{g}} \geq (M^{bb}_{inv})^{kink} + m_{\tilde{\chi}^0}$. Embedded window shows mass distributions for SUSY and SM with a 200 GeV E_T^{miss} cut. To suppress SM background take (i) a 400 GeV E_T^{miss} cut, (ii) two more jets besides 2 b-tagged jets.

Monojet Signatures

Feldman, Liu, PN, Nelson, PRD 80, 075001 (2009)

	HWM		PWM	
Object Cuts (GeV)	Events	$S/\sqrt{B}$	Events	$S/\sqrt{B}$
$p_T^{\rm jet} \geq 150$, $\not{E}_T \geq 150$	1994	2.13	3442	3.68
$p_T^{\rm jet} \geq 200$, $\not{E}_T \geq 150$	1302	2.52	1983	3.84
$p_T^{\rm jet} \geq 150$, $\not{E}_T \geq 200$	1334	2.53	2147	4.08
$p_T^{\rm jet} \geq 200$, $\not{E}_T \geq 200$	1241	2.58	1904	3.95
$p_T^{\rm jet} \geq 150$, $\not{E}_T \geq 300$	659	3.57	771	4.17

Table: Monojet signature for the HWM and the PWM: Event counts are after 100 fb^{-1} of integrated luminosity for various choices of cuts on total $\not{E}_T$ and jet p_T. All signatures involve a lepton veto and require no other jets in the event with $p_T^{\rm jet} \geq 20$ GeV. No transverse sphericity cut was applied in any of these signatures.

Multicomponent dark matter

Feldman, Liu, PN, Peim, arXiv:1004.0649
PRD to appear

Various other works on multicomponent DM
JE Kim
Cirelli, Cline

Dark matter may be constituted of more than one component.

$$\Omega_{CDM}h^2 = \sum_i \Omega_{CDM\,i}h^2.$$

$U(1)_X \times U(1)_C$ extension where $U(1)_X$ is hidden sector and $U(1)_C$ is the anomaly free combination $L_e - L_\mu$.

$$\mathcal{L} = \mathcal{L}_{\rm MSSM} + \mathcal{L}_{U(1)^2} + \Delta\mathcal{L},$$

where $\mathcal{L}_{U(1)^2}$ is the kinetic energy for the X and C multiplets and for $\mathcal{L}_{\rm St}$ we assume the following form

$$\Delta\mathcal{L} = \int d^2\theta d^2\bar{\theta}\ [(M_1C + M_2'X + S + \bar{S})^2\ + (M_1'C + M_2X + S' + \bar{S}')^2].$$

A Dirac fermion is placed in the hidden sector. The new particles in this model consist of

$$\text{spin } 0 : \rho, \rho', \phi, \phi'$$
$$\text{spin } \frac{1}{2} : \psi, \chi_5^0, \chi_6^0, \chi_7^0, \chi_8^0$$
$$\text{spin } 1 : Z', Z''.$$

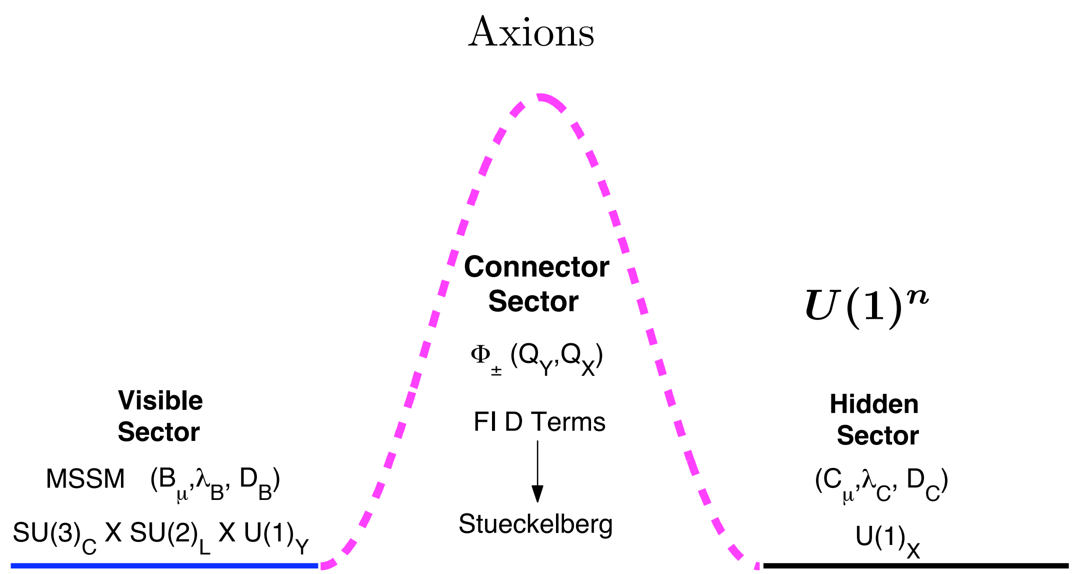

Mixing between U_X(hidden) and U_Y (hypercharge) as a probe of the hidden sector was introduced in Kors, PN, Phys.Lett.B586:366-372,2004.

Hidden Sector and Leptophilic Couplings

The basic interaction of X_μ and of C_μ with matter is given by

$$\mathcal{L}_{int} = g_X Q_X \bar{\psi}\gamma^\mu \psi X_\mu + \sum_f g_C Q_C^f \bar{f}\gamma^\mu f C_\mu$$

where f runs over e and μ families and where $Q_C^e = -Q_C^\mu$. In the mass diagonal basis the interaction assumes the form

$$\begin{aligned}\mathcal{L}_{int} = &(g_X Q_X \bar{\psi}\gamma^\mu \psi \cos\theta_X - \sum_f g_C Q_C^f \bar{f}\gamma^\mu f \sin\theta_X) Z'_\mu \\ &+ (g_X Q_X \bar{\psi}\gamma^\mu \psi \sin\theta_X + \sum_f g_C Q_C^f \bar{f}\gamma^\mu f \cos\theta_X) Z''_\mu.\end{aligned}$$

These interactions lead to the annihilation of $\psi\bar{\psi}$ into e^+e^- and $\mu^+\mu^-$ via the Z', Z'' poles for which we assume Breit-Wigner forms.

Z' and Z'' resonances

The partial Z', Z'' decay widths

$$\Gamma(Z' \to f\bar{f}) = (g_C Q_C^f \sin\theta_X)^2 \frac{M_{Z'}}{12\pi},$$
$$\Gamma(Z'' \to f\bar{f}) = (g_C Q_C^f \cos\theta_X)^2 \frac{M_{Z''}}{12\pi},$$

$$\Gamma(Z' \to \psi\bar{\psi}) = (g_C Q_C^f \cos\theta_X)^2 \frac{M_{Z'}}{12\pi}(1 + \frac{2M_\psi^2}{M_{Z'}^2})(1 - \frac{4M_\psi^2}{M_{Z'}^2})^{1/2}\Theta(M_{Z'} - 2M_\psi)$$

and similarly for the partial decay width of the Z'' into $\psi\bar{\psi}$ with $M_{Z'} \to M_{Z''}$ and $\cos\theta_X \to \sin\theta_X$.

- For small mixing angle θ_X Z' decay width into $f\bar{f}$ is much smaller than the Z'' decay width into $f\bar{f}$.
- If $M_\psi \simeq M_{Z'}/2$, the Z' decay width into $\psi\bar{\psi}$ will be small due to kinematical suppression while the Z'' decay width into $\psi\bar{\psi}$ will be small due to mixing angle.
- The above results in Z' to be a narrow resonance.

Constraints from $g_\mu - 2$

Their exchange gives

$$\Delta(g_\mu - 2) = \frac{g_C^2 m_\mu^2}{24\pi^2}\left[\frac{\sin^2\theta_X}{M_{Z'}^2} + \frac{\cos^2\theta_X}{M_{Z''}^2}\right].$$

The current error is

$$\Delta(g_\mu - 2) = 1.2 \times 10^{-9}$$

in the determination of $g_\mu - 2$.
Assuming θ_X is small, one finds the following constraint on α_C,

$$\alpha_C \lesssim 0.001\left(\frac{M_{Z''}}{300\ \mathrm{GeV}}\right)^2 ,$$

where $\alpha_C = g_C^2/4\pi$. Precision electroweak fits are unaffected.

Dark matter possibilities in the $U(1)_X \times U(1)_C$ extension.

- Two component dark matter: Dirac (ψ), Majorana (χ).
- Three component dark matter: Dirac (ψ), scalars (ϕ, ϕ').
- Four component dark matter:Dirac (ψ), Majorana (χ) and scalars ($\phi, \phi',$).

Two component dark matter: ψ and χ

$$\psi + \bar{\psi} \to Z, Z', \gamma \to \mathrm{SM} + \mathrm{SM}',$$

$$\chi + \chi \to (s : Z', Z, h, H, A, \rho), (t/u : \tilde{f}_a, \chi_i, \chi_k^{\pm}) \\ \to \mathrm{SM} + \mathrm{SM}' + \text{plus coannihilations}$$

Boltzmann equations for the two component model

$$\frac{dn_\psi}{dt} = -3Hn_\psi - \frac{1}{2}\langle\sigma v\rangle_{\psi\bar{\psi}}(n_\psi^2 - n_{\psi,\mathrm{eq}}^2), \quad (3)$$

$$\frac{dn_\chi}{dt} = -3Hn_\chi - \langle\sigma v\rangle_{\chi\chi}(n_\chi^2 - n_{\chi,\mathrm{eq}}^2) + \frac{1}{2}\langle\sigma v\rangle_{\psi\bar{\psi}\to\chi\chi}(n_\psi^2 - n_{\psi,\mathrm{eq}}^2).$$

Here $\langle\sigma v\rangle_{\psi\bar{\psi}}$ refers to $\psi\bar{\psi} \longrightarrow f\bar{f}, \chi\chi$, and $\langle\sigma v\rangle_{\chi\chi}$ stands for $\langle\sigma v\rangle_{\chi\chi\to\mathrm{SM\ SM'}}$.

Total relic density

$$(\Omega h^2)_{\mathrm{WMAP}} = (\Omega_\psi h^2)_0 + (\Omega_\chi h^2)_0 \simeq \frac{C_\psi}{J_0^\psi} + \frac{C_\chi}{J_0^\chi},$$

$$C_\chi \simeq \frac{1.07\times 10^9\ \mathrm{GeV}^{-1}}{\sqrt{g^*(\chi)}M_{\mathrm{pl}}}, \quad C_\psi \simeq 2\times\frac{1.07\times 10^9\ \mathrm{GeV}^{-1}}{\sqrt{g^*(\psi)}M_{\mathrm{pl}}},$$

$$J_0^\chi = \int_0^{x_f^\chi}\langle\sigma v\rangle_{\chi\chi}\,dx, \qquad J_0^\psi = \int_0^{x_f^\psi}\langle\sigma v\rangle_{\psi\psi}\,dx.$$

The local density of dark matter

$$\rho_{\odot,\psi}/\rho_{\odot,\chi} \sim (\Omega_\psi h^2)_0/(\Omega_\chi h^2)_0.$$

Multi-component Dark Matter

Feldman, Liu, PN, Peim arXiv:1004.0649000

Positron flux

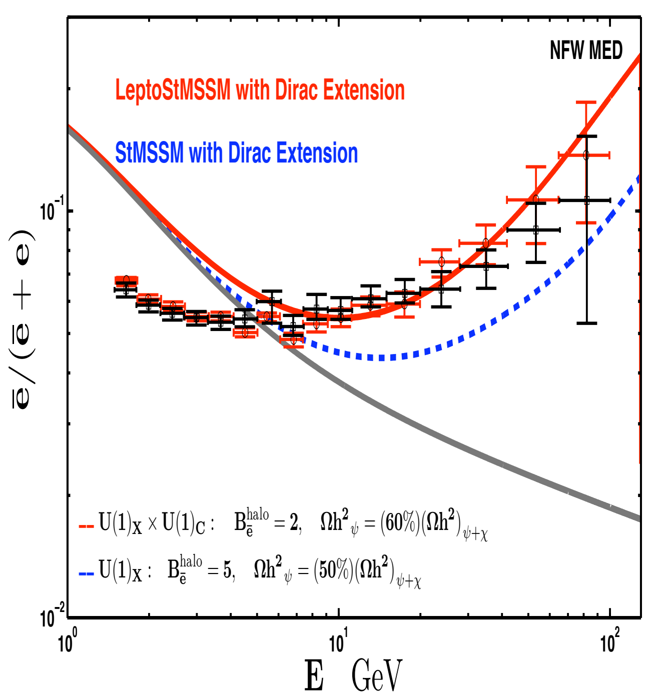

$\bar{p}$ flux

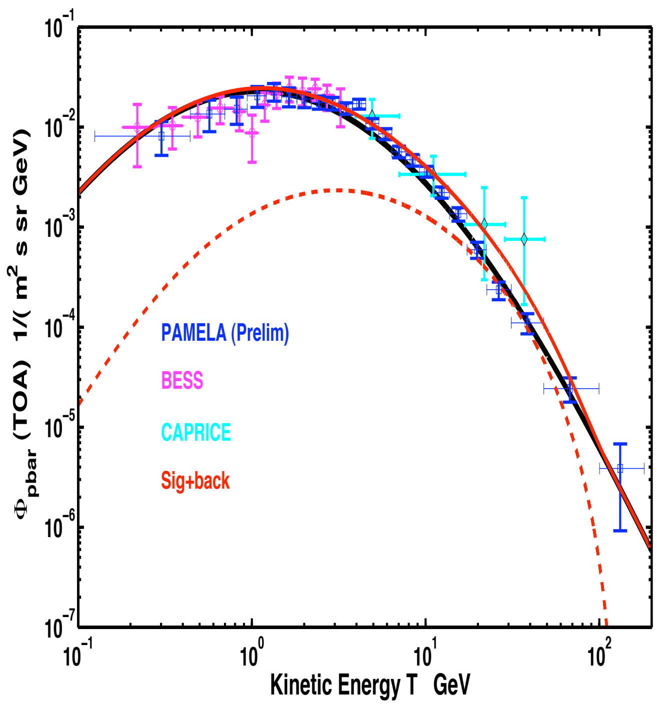

Two-component Dark Matter Model

Feldman, Liu, PN, Peim arXiv:1004.0649000

Photon flux

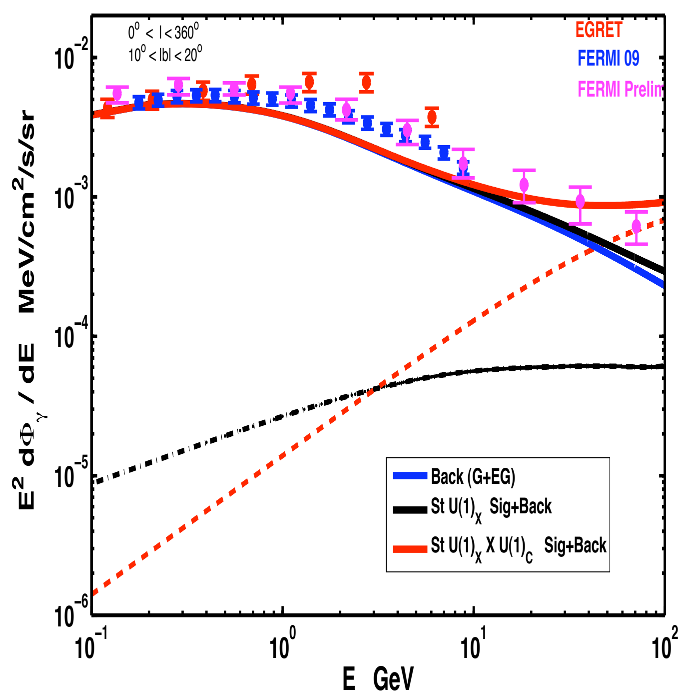

σ_{SI}

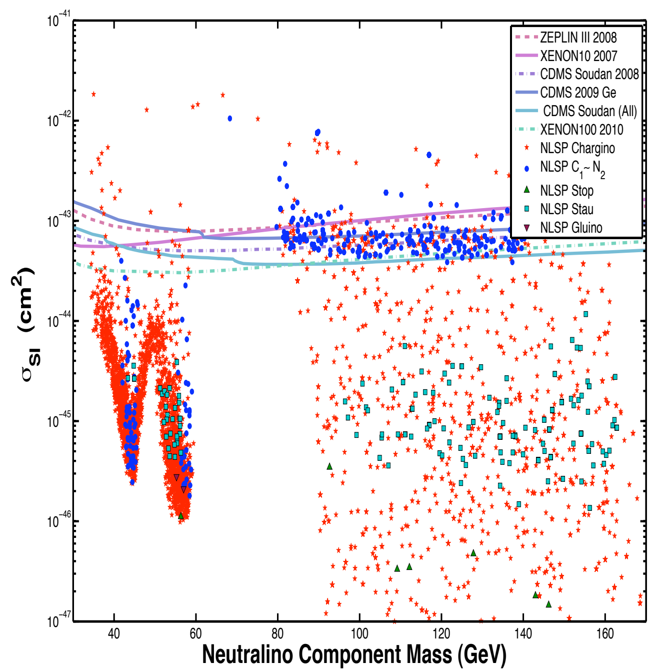

How large a spin independent cross section in neutralino proton scattering?

Explore the cross sections under the following set of constraints

- Radiative electroweak symmetry breaking constraint (REWSB)
- Relic density constraint
- Experimental constraints on sparticle masses, FCNC constraints etc.

One finds that REWSB constraints by themselves allow σ_{SI} as large as 10^{-40} cm^{-2} or even larger. However, the cross sections are cut down under the relic density and other experimental constraints. Specifically it is difficult to get $\sigma_{SI} \sim 10^{-40}$ cm^{-2} at $m_\chi = 10$ GeV with all the experimental constraints imposed.

COGENT

Feldman, Liu, PN arXiv: 1003.0437, PRD to appear

Also: Kuflick, Pierce, Zurek

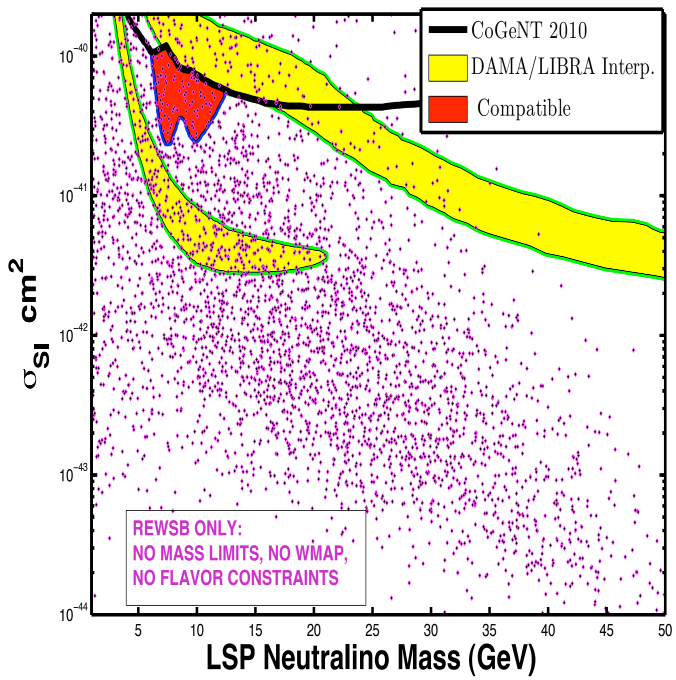

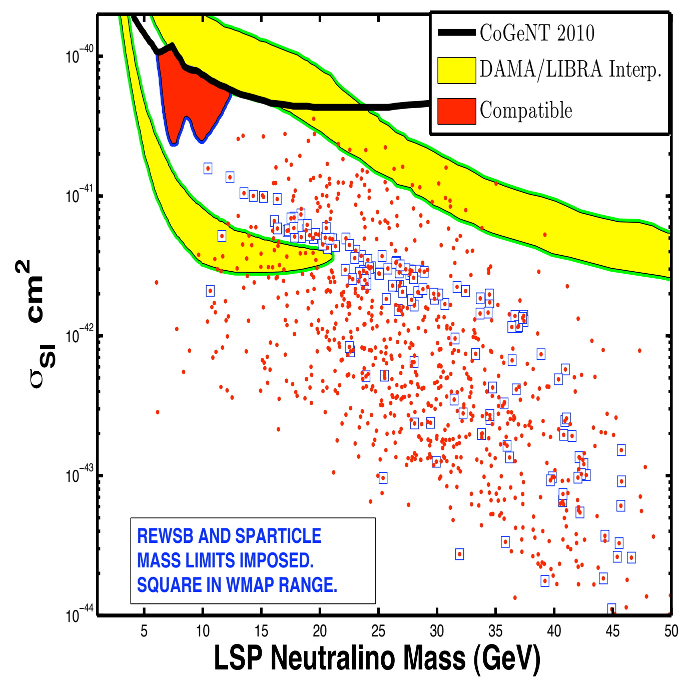

Difficult to get 10^{-40} cm^2 at $m_\chi = 10$ GeV with REWSB and experimental constraints.

Conclusions

- The LHC data will be very helpful in establishing the early history of the universe, e.g., whether dark matter originated via stau co-annihilation or on the hyperbolic branch, or by some other mechanism.
- Dark matter experiments along with LHC data will help decipher the nature of dark matter including if it is constituted of one or more than one components.

Extra Transparencies

Positron excess vs WMAP

The basic issue: one needs $< \sigma v > \sim 10^{-24} cm^3/s$ for positron excess and $< \sigma v > \sim 10^{-26} cm^3/s$ for relic density. Different possibilities

- Breit-Wigner pole enhancement of $< \sigma v >$ in the galaxy
  Feldman, Liu, PN; Ibe, Murayama, Yanagida
- The Boost from Coannihilation (B_{Co}) mechanism to enhance relic density
  Feldman, Liu, PN, Nelson
- Sommerfeld enhancement
- Non-thermal processes to enhance relic density.

Enhancement of annihilation cross section in the galaxy

Feldman, Liu, PN, PRD 79, 063509 (2009)